Title
Designer receptors show role for ventral pallidum input to ventral tegmental area in cocaine seeking

Journal
Nature Neuroscience, 17(4)

ISSN
1097-6256

Authors
Mahler, Stephen V
Vazey, Elena M
Beckley, Jacob T
et al.

Publication Date
2014-04-01

DOI
10.1038/nn.3664

HHS Public Access

Author manuscript

Nat Neurosci. Author manuscript; available in PMC 2014 October 01.

Published in final edited form as:

Nat Neurosci. 2014 April ; 17(4): 577–585. doi:10.1038/nn.3664.

Designer Receptors Show Role for Ventral Pallidum Input to Ventral Tegmental Area in Cocaine Seeking

Stephen V. Mahler[1], **Elena M. Vazey**[1], **Jacob T Beckley**[1], **Colby R. Keistler**[1], **Ellen M. McGlinchey**[1], **Jennifer Kaufling**[1], **Steven P. Wilson**[2], **Karl Deisseroth**[3], **John J. Woodward**[1], and **Gary Aston-Jones**[1]

[1]Department of Neurosciences, Medical University of South Carolina. 173 Ashley Ave, 409 BSB. Charleston, SC 29425

[2]Department of Pharmacology, Physiology and Neuroscience, School of Medicine, University of South Carolina. 6311 Garners Ferry Rd, Columbia, SC, 29208

[3]Department of Bioengineering and Psychiatry and Behavioral Sciences, 318 Campus Drive West Clark Center W083. Stanford University. Stanford, CA 94305

Abstract

Ventral pallidum (VP) is centrally positioned within mesocorticolimbic reward circuits, and its dense projection to ventral tegmental area (VTA) regulates neuronal activity there. However, VP is a heterogeneous structure, and how this complexity affects its role within wider reward circuits is unclear. Here we demonstrate that projections to VTA from rostral (RVP), but not caudal VP (CVP) are robustly Fos-activated during cue-induced reinstatement of cocaine seeking—a rat model of relapse in addiction. Moreover, designer receptor-mediated transient inactivation of RVP neurons, their terminals in VTA, or functional connectivity between RVP and VTA dopamine neurons blocks the ability of drug-associated cues (but not a cocaine prime) to reinstate cocaine seeking. In contrast, CVP neuronal inhibition instead blocked cocaine-primed, but not cue-induced reinstatement. This novel double dissociation in VP sub-regional roles in drug seeking is likely important for understanding mesocorticolimbic circuits underlying reward seeking and addiction.

Ventral pallidum (VP) is a crucial node in ventral striatopallidal circuits underlying reward-related behaviors, with major reciprocal connections to accumbens, extended amygdala, limbic thalamus, substantia nigra (SN) and ventral tegmental area (VTA)[1–4]. VP neurons respond to rewards and their cues in animals and humans, and are necessary for reward-

Author Contributions: SVM attained funding, designed and conducted experiments, performed surgeries, analyzed data, and wrote the manuscript. EMV designed and conducted anesthetized electrophysiology experiments, analyzed these data, and wrote the manuscript. JTB designed and conducted slice electrophysiology experiments, analyzed these data, and wrote the manuscript. CRK conducted behavioral experiments and wrote the manuscript. EMM performed surgeries for, and conducted behavioral and immunohistochemical experiments. Jennifer Kaufling conducted immunohistochemical and confocal microscopy experiments. SPW attained funding, and contributed the *Syn-GFP* viral construct. KD contributed the TH::Cre transgenic rat line. JJW attained funding, designed and conducted slice electrophysiology experiments and wrote the manuscript. GA-J attained funding, designed experiments, and wrote the manuscript.

seeking behaviors—leading to hypotheses that VP helps translate motivational states into appetitive behaviors[5–7].

However, VP is a heterogeneous structure, exhibiting medial-lateral and rostral-caudal variation in histological markers and connectivity patterns[1, 4, 8]. Notably, ventromedial VP (most of which is located subcommissurally, rostral of bregma in rat: RVP) receives dense afferents from nucleus accumbens shell, and projects strongly to mediodorsal thalamus and VTA. Dorsolateral VP (most of which is located sublenticularlly, caudal of bregma: CVP) instead receives afferents from accumbens core, and projects to SN and subthalamic nucleus (STN), in addition to VTA[1, 9]. This topography implies involvement of VP subregions in functionally distinct mesolimbic circuits.

Functional heterogeneity between VP subregions has also been reported. In vitro, RVP and CVP neurons differ in several ways; many RVP neurons have spiny dendrites, glutamatergic afferents, hyperpolarized membrane potentials, and no spontaneous action potentials[10]. Intriguingly, these characteristics are more typical of accumbens medium spiny neurons than “classical” VP neurons. In contrast, CVP neurons have more “classical” pallidal characteristics, including aspiny dendrites, GABAergic inputs, depolarized membrane potentials, and spontaneous action potentials. Notably, neuronal firing during rat cocaine self-administration varies depending on mediolateral and rostrocaudal localization within VP[11], and VP rostrocaudal variation exists in neuronal cytoarchitecture, in vivo firing rates, sensitivity to rewarding effects of electrical stimulation and microinjected drugs, opioid agonist-induced hedonic responses to tastes, and fMRI activation to emotionally arousing pictures[12–19].

However, little is known about how such heterogeneity contributes to VP functions within wider mesolimbic circuits. In rat, CVP provides tonically-active GABA inputs to VTA and SN that gate firing of subpopulations of dopamine neurons and modulate reward seeking[20]. However, VP neurons are also acutely activated by reward-associated cues[6, 21, 22], and VP projections to VTA are activated during cue-induced reinstatement of cocaine seeking[23]. How does functional-anatomical heterogeneity impact VP regulation of VTA, and the role of this circuit in drug seeking?

We sought to examine the roles of VP subregions and their VTA projections in relapse to cocaine seeking. We examined Fos activation of RVP and CVP projections to VTA, and inactivated these subregions or their projections to midbrain dopaminergic regions during reinstatement of cocaine seeking using Designer Receptors Exclusively Activated by Designer Drugs (DREADDs)[24]. DREADDs utilize endogenous G-protein signaling pathways, but do not affect neuronal activity in the absence of their otherwise inert, exogenously-administered ligand, clozapine-n-oxide (CNO). The G_i-coupled (hM4Di) DREADDs used here thereby allow transient inactivation of defined neuronal populations[25]. We also show that they can be used to manipulate axonal terminals of DREADD-expressing neurons to inactivate particular monosynaptic pathways (e.g. RVP-VTA), or to disrupt functional connectivity between specific neuronal populations (e.g. RVP and VTA dopamine neurons). We demonstrate a novel double-dissociation between rostral and caudal VP in cued vs. cocaine primed reinstatement respectively, and show that cued cocaine

seeking is dependent upon RVP projections to VTA, and complex interactions with dopaminergic and non-dopaminergic neurons there.

Results

Validation of VP DREADDs

We used a DREADD-based strategy to remotely control VP neurons *in vivo* and manipulate the VP-VTA circuit. We injected a synapsin-driven lentiviral vector yielding expression of the G_i-coupled DREADD, hM4Di[24], or a control virus lacking the DREADD gene (*Syn-GFP*) into RVP or CVP, and allowed animals to survive 6+ weeks before analyzing brain tissue for virus expression. The S*yn-hM4Di-HA-GFP* virus (Fig. 1a) caused robust hM4Di expression within RVP or CVP [visualized with immunoreactivity for the hemagglutinin (HA) tag, or green fluorescent protein (GFP) reporter]. These injections yielded limited expression outside the borders of VP (<30% labeling outside VP borders; Figs.1b–e, 2d, Supplemental Fig. 1). S*yn-hM4Di-HA-GFP* and *Syn-GFP* viruses yielded comparable zones of somatic GFP or hM4Di expression centered at the injection site [GFP: 0.82(0.21) mm^3; hM4Di: 0.89(0.05) mm^3].

We then used *in vivo* electrophysiology to functionally validate hM4Di receptor expression. In isofluorane-anesthetized rats, local CNO microinjection (60 nl,100 μM) inhibited VP neurons (n=24 cells; m=60.3 ± 6.6% decrease in firing; Z = −2.54; p=0.011; Fig. 1f–g). Local CNO similarly affected RVP (11/13 cells inhibited) and CVP (8/11 inhibited) neurons, with 58.2 ± 8.7% and 63.2 ± 10.6% inhibition, respectively. Pre-CNO firing rates in RVP (m=6.4 ± 2.0 Hz) were lower than in CVP (m=24.8 ± 5.3 Hz; p=0.007; t_{12}=3.26), as previously reported[10, 12].

Double Dissociation of VP Subregion Roles in Reinstatement

Next, we examined whether transient DREADD-mediated inhibition of RVP or CVP would attenuate either cued or cocaine primed (10 mg/kg) reinstatement of cocaine seeking following cocaine self-administration and extinction (Fig. 2a). CNO (0,0.1,1,10, or 20 mg/kg) attenuated cued reinstatement in rats with hM4Di expression in RVP, but not in animals with comparable DREADD expression in CVP [RVP (n=16 rats): $F_{4,39}$=4.0, p=0.008; CVP (n=17 rats): $F_{4,46}$=0.59, *n.s.*; Fig. 2b]. In contrast, CNO (0, 10 or 20 mg/kg) injections attenuated cocaine-primed reinstatement only in animals with hM4Di expression in CVP, but not in RVP (RVP: $F_{2,29}$=0.45, *n.s.*; CVP: $F_{2,31}$=3.48, p=0.04; Fig. 2c), revealing a novel double-dissociation between RVP and CVP for reinstatement elicited by cues vs. cocaine.

The zones in which hM4Di inhibition were most effective at reducing cued reinstatement were centered in RVP, while effective sites for cocaine-primed reinstatement were centered in CVP (cue—VP site x drug interaction: $F_{1,16}$=7.35, p=0.015; prime—VP site x drug interaction: $F_{1,25}$=4.85, p=0.037). VP inhibition was sufficient for these effects, as cases with minimal (<5%) hM4Di expression outside VP borders showed equivalent reinstatement effects as those with more (<30%) encroachment of expression into adjacent areas (Supplemental Fig. 1). CNO had no effects in animals with either GFP virus injections (*Syn-*

GFP, lacking the hM4Di gene; n=5 rats; cue: $F_{2,11}$=0.58, *n.s.*; prime: $F_{1,8}$=0.05, *n.s.*), or no virus expression (n=9 rats; cue: $F_{2,18}$=0.87, *n.s.*; prime: $F_{2,24}$=0.28, *n.s.*; control groups combined: cue: $F_{2,28}$=0.77, *n.s.*; prime: $F_{2,31}$=0.22, *n.s.*; Fig. 2b–c)].

Fos Activation of RVP-VTA Projections During Reinstatement

We next asked whether the role for RVP in cued reinstatement behavior involves projections to VTA. First, we examined Fos expression in RVP or CVP VTA-projecting neurons during cued reinstatement, or control behaviors (Fig. 3a; Supplemental Fig. 2). The retrograde tracer cholera toxin beta subunit (CTb) was injected into rostral or caudal VTA. Animals (n=25) were trained to self-administer *i.v.* cocaine+cues, extinguished, then given a 2 h cue-induced reinstatement test or control behavioral test, as described in Online Methods. Animals were sacrificed immediately after this test session, and VP slices were co-stained for Fos and CTb.

In RVP, VTA-projecting (CTb+) neurons were Fos-activated during cued cocaine seeking (CS+, n=8 rats), but not during exposure to the extinguished self-administration chamber (Ext., n=7), a novel environment (Loco, n=6), or a familiar, non-cocaine associated CS− stimulus (CS−, n=4; $F_{3,21}$=6.6, p=0.002; Fig. 3c). Unlike RVP, CVP projections to VTA were not specifically activated during cued reinstatement ($F_{3,21}$=2.3, *n.s.*; Fig. 3c; Supplemental Fig. 2). Moreover, in individual CS+ animals, the degree of Fos activation of VTA afferents from RVP, but not CVP was positively correlated with the degree of cue-induced cocaine seeking behavior (RVP: r=0.78, p=0.02; CVP: r=−0.54, *n.s.*; Fig. 3d; Supplemental Fig. 2d), indicating that more activity in RVP efferents to VTA is associated with more cue-triggered drug seeking.

Validating Inhibition of RVP-VTA Projection with DREADDs

The hM4Di DREADD is trafficked axonally, evidenced by numerous HA+ fibers and terminals reliably observed in ventral midbrain after hM4Di vector injection in RVP or CVP (Fig. 3b,4a, Supplemental Fig. 3d–e). We examined whether modulation of G_i-coupled signaling in VP axon terminals in VTA via local CNO application would alter activity of VTA neurons. First, we recorded spontaneous inhibitory postsynaptic currents (sIPSCs) from dopamine neurons (verified by tyrosine hydroxylase (TH) immunoreactivity) in VTA slices from rats that were injected 6+ weeks prior with the hM4Di vector in RVP (n=7 rats; Fig. 4b–c). Perfusion with 5 μM CNO had no effect on sIPSC amplitude (t_6=0.94, *n.s.*; Fig. 5d), but decreased frequency (t_6 = 2.50, p=0.046) and shifted the cumulative distribution of inter-event intervals (IEIs) to the right (main effect of IEI duration: $F_{21,264}$=22.18, p=0.0001; and CNO treatment: $F_{1,264}$=14.42, p=0.0002; Fig. 4e). In slices from *Syn-GFP* injected animals (n=5 cells), which also expressed GFP in RVP neurons and their VTA axons, CNO had no effect on sIPSC amplitude (t_4 = 0.47, *n.s.*) or IEIs (t_4 = 0.39, *n.s.*; Supplemental Fig. 4). These findings indicate that activation of hM4Di DREADDs on VP terminals in VTA decreased GABA release onto VTA dopamine neurons.

We confirmed this finding *in vivo*, demonstrating that intra-VTA CNO microinjection in RVP-hM4Di rats significantly increased firing rate (m=82.5 ± 50.2% increase) in 8 of 9 “Type 1 neurons” (those meeting conventional electrophysiological criteria for VTA

dopamine neurons[26]; p=0.03; t_7 = 2.63; Fig. 4f–g). Conversely, 10 of 14 fast-spiking, short-waveform "Type 2" VTA neurons (not conventionally dopamine-like) were inhibited (m= −60.5 ± 12.0% change in discharge) after intra-VTA microinjection of CNO in RVP-hM4Di rats (p=0.003; t_9 = 3.93; Fig. 4h–i).

Inhibiting RVP Terminals in VTA Blocks Cued Reinstatement

Next, we examined effects of inactivating VP terminals in VTA on cued or cocaine-primed reinstatement behavior. RVP hM4Di animals (n=28) were microinjected (in counterbalanced order on separate days) with CNO (1 mM/0.3 μl/side) or vehicle (artificial cerebrospinal fluid: aCSF) into VTA (n=17 rats) or SN (n=11), 5 min prior to cued or primed reinstatement (2 tests each/animal; Fig. 5a). CVP hM4Di animals (n=9) were also injected with CNO (0&1 mM/0.3 μl) into VTA, then tested on cued or primed reinstatement (Fig. 5a; cannulae sites in Supplemental Fig. 5). Inhibition of RVP terminals in VTA with local CNO selectively attenuated cued, but not primed reinstatement (cue: $F_{1,16}$=27.87, p=0.000075; prime: $F_{1,16}$=0.01, *n.s.*; Fig. 5b), indicating that activation of the RVP projection to VTA is required for drug cues to drive reinstatement of cocaine seeking. In contrast, inactivating RVP terminals in SN, or CVP terminals in VTA, had no effects on cued or primed reinstatement (RVP-SN inhibition, cue: $F_{1,10}$=0.21, *n.s.*, prime: $F_{1,10}$=0.01, *n.s.*; CVP-VTA inhibition, cue: $F_{1,8}$=0.84, *n.s.*, prime: $F_{1,8}$=0.37, *n.s.*; Fig. 5d,f). This indicates that although CVP is necessary for cocaine-primed reinstatement (Fig. 2c), its VTA targets are not essential for this action.

Inactivating RVP projections to VTA in the absence of cues or priming injections failed to affect drug seeking following extinction (n=4 rats; vehicle AL presses m±SEM=8.7±6.7, CNO m=4.3±1.7; $F_{1,3}$=3.9, *n.s.*). In RVP (n=11) or CVP (n=6) hM4Di animals, neither intra-VTA (n=17) nor intra-SN (n=6) CNO had significant effects on general locomotor behavior in a familiar environment (no main effect of drug or drug X time interactions; Fs<1.7, *n.s.*; Fig. 5c,e,g), indicating that reinstatement effects of RVP-VTA inhibition are more likely motivational than motoric in nature.

RVP Interacts with VTA Dopamine Neurons in Reinstatement

VTA is a complex structure, with dopamine, GABA and glutamate projection neurons, as well as interneurons and other local connectivity[27–31]. Because VP projections modulate dopamine and non-dopamine neuron firing in VTA[32] (Fig. 4), we asked whether reinstatement behavior is affected by contrahemispheric disconnection of RVP from VTA dopamine neurons. In transgenic rats that express Cre recombinase in TH neurons (TH::Cre + rats)[33], we unilaterally transduced RVP neurons with the S*yn-hM4Di-HA-GFP* lentivirus described above. We also injected a double-floxed hM4Di AAV virus (*DIO-Syn-hM4Di-mCherry*; Fig. 6a) into the contralateral VTA (n=9 rats) or SN (n=8), yielding reliable and anatomically restricted hM4Di expression in unilateral dopamine neurons (Fig. 6b–c; Supplemental Fig. 6). A systemic CNO injection in these animals therefore functionally disconnected RVP inputs from midbrain dopamine cells bilaterally, while sparing RVP connectivity with non-dopaminergic VTA neurons (Fig. 6d). Control groups consisted of Cre+ animals with unilateral VTA *DIO-Syn-hM4Di-mCherry* injections but no virus in RVP

(n=6 rats), or Cre− littermates (n=10) with unilateral RVP hM4Di and contralateral VTA injections of *DIO-Syn-hM4Di-mCherry* (but no VTA hM4Di expression).

As shown in Fig. 6, cue-induced reinstatement was markedly attenuated by disrupting the RVP-VTA dopamine circuit in this manner ($F_{1,8}$=37.97, p=0.0003; Fig. 6e). No effects were found after similarly disconnecting RVP from SN dopamine neurons ($F_{1,7}$=0.29, *n.s.*), or after unilaterally inactivating either RVP ($F_{1,9}$=0.06, *n.s.*) or VTA dopamine neurons ($F_{1,5}$=0.57, *n.s.*; Fig. 6e). This indicates that intact connectivity between RVP (not CVP) and VTA (not SN) dopamine populations is required for conditioned cues to trigger cocaine seeking during reinstatement.

Further Examinations of the Nature of the RVP-VTA Circuit

GABAergic VP projections to VTA can tonically inhibit VTA dopamine neurons[5], and inactivating this projection with DREADDs can disinhibit dopamine neurons (Fig. 4). We therefore asked if disinhibition of VTA dopamine neurons could have contributed to the attenuation of reinstatement we observed after inactivating RVP inputs to VTA with DREADDs. If so, then direct disinhibition of VTA dopamine neurons with the $GABA_A$ antagonist gabazine should also attenuate reinstatement. Instead, we observed that intra-VTA gabazine (10 μM/0.3 μl) strongly increased cued reinstatement (n=6 rats; $F_{2,17}$=9.43, p=0.002; veh vs. 10 μM gabazine active lever: t_6=2.62, p=0.04; Fig. 7g–h), and robustly induced Fos in nearby dopamine neurons (veh n=3, gabazine n=5 rats; no effect on number of TH+ cells: t_6=0.2, n.s.; total Fos+ TH+ cells: $t_{4.4}$=5.55, p=0.001; percent Fos+ TH cells: t_6=8.84, p=0.0001; Fig. 7a–f). This indicates that simple disinhibition of dopamine neurons is not likely the mechanism by which inhibiting RVP inputs to VTA reduces cued reinstatement.

In addition to GABA projections, RVP sends numerous VGlut2+ efferents to VTA[34]; we asked whether this glutamatergic projection is required for cued reinstatement. We used unilateral DREADD-based RVP inhibition and contralateral VTA microinjection of a cocktail of the AMPA/NMDA antagonists CNQX/AP5 (0.7/1.6 mM) to bilaterally compromise glutamate projections from RVP to VTA. This did not affect cued reinstatement (n=5 rats; t_4=1.28, *n.s.*; Supplemental Fig. 7). In contrast, reinstatement was attenuated when all VTA neurons (baclofen/muscimol; 0.3/0.03 mM) were inhibited contralaterally to a DREADD-inactivated RVP (RVP/VTA disconnect, n=10 rats: t_9=2.81, p=0.02; no effect of unilateral VTA baclofen/muscimol alone, n=8: t_7=1.03, *n.s.*; Supplemental Fig. 7). In slice, we also explored whether inhibiting RVP inputs to VTA would decrease spontaneous excitatory transmission (sEPSCs) onto dopamine neurons. CNO (5 μM) had no effects on sEPSC amplitude (t_5=0.22, *n.s.*) or frequency (t_5=0.43, *n.s.*) in TH+ cells (n=6 cells, Supplemental Fig. 8). These findings indicate that RVP glutamatergic projections to VTA do not directly modulate dopamine neurons, nor are they likely to be necessary for cued reinstatement.

Discussion

Here, we describe an RVP-VTA pathway activated by, and necessary for, conditioned cue-induced reinstatement of cocaine seeking in rats. VP's involvement in reinstatement depends

critically upon both the rostrocaudal position within VP, and the means by which drug seeking is reinstated (cues vs. cocaine prime). Cue-triggered drug seeking specifically requires both RVP projections to VTA, and functional interactions between RVP inputs and VTA dopamine and non-dopamine neurons. In addition to describing a novel double dissociation between VP subregions in drug seeking, we also validate the use of G_i-coupled DREADDs to inactivate specific neuronal pathways via modulation of DREADD-expressing terminals, and to functionally disconnect brain circuits in vivo.

VP Roles in Reward Seeking—Much prior research has focused on the portion of VP caudal of bregma in rat (CVP), which showed that VP is an important node in mesocorticolimbic reward circuits. Lesions or pharmacological inactivation of CVP reduce drug- or food-seeking[13, 35–38]. Many of these VP neurons are spontaneously active, and their GABAergic projection to VTA tonically inhibits populations of dopamine neurons there[5].

VP efferents to VTA are also acutely activated by rewards and associated cues. For example, VP-VTA projections in rats are Fos-activated after acute amphetamine, cocaine self-administration, or cued reinstatement of cocaine seeking[23, 39, 40], and VP neurons phasically fire when salient rewards and their cues are experienced[6, 11]. In primates, VP neurons also fire in relation to reward anticipation, and VP inactivation compromises modulation of reward seeking based upon reward expectation[22]. Similarly, VP is fMRI-activated by cues for drug or natural rewards in humans[41]. Our report therefore supports, and substantially expands upon the known roles for VP in reward-seeking.

Anatomical and Functional Heterogeneity Within VP—Anatomically, both rostrocaudal and mediolateral heterogeneity exists in VP cell morphology, transmitter content, sources of afferents, and efferent targets[6, 10, 16, 42, 43]. A large proportion of subcommissural RVP consists of a neurotensin-positive, ventromedial subregion, which receives afferents from medial accumbens shell, and sends efferents to mediodorsal thalamus and VTA. In contrast, a large proportion of sublenticular CVP consists of a calbindin-positive, dorsolateral subregion that receives accumbens core inputs, and projects to SN and subthalamic nucleus[1]. RVP (and adjacent caudal accumbens shell) has been described as a transition zone between accumbens and traditional (caudal) VP, with connectivity and morphological features distinct from rostral accumbens, pallidal, or extended amygdala regions[10, 42]. Supporting this view, RVP and caudal ventromedial accumbens shell project similarly to VTA, and Fos activation of both projections is correlated with cue-induced reinstatement behavior (Fig. 3)[23].

Previous evidence supports a role for RVP in conditioned motivation, and CVP in the rewarding and priming effects of reinforcers themselves. For example, RVP (but not CVP) is Fos-activated during motivated behaviors triggered by Pavlovian cues for specific salient rewards, and is necessary for these cues to trigger seeking behaviors[44, 45]. RVP (not CVP) is fMRI-activated when people view highly salient, disgusting photographs—again indicating a role in conditioned motivational states[18]. In contrast, GABA agonists microinjected into CVP reduce cocaine-primed and stress-induced reinstatement of cocaine seeking[35, 36], aligning with our observation that DREADD-based inhibition of CVP neurons blocked

primed reinstatement (although ours is the first report for a role of VP, more specifically RVP, in cued reinstatement of cocaine seeking). Additionally, CVP (not RVP) has been linked to the hedonic evaluation of primary rewards in animals and humans[18, 19].

Here, we examined the functions of RVP and CVP in cued vs. primed reinstatement of cocaine seeking. We showed that RVP (not CVP) is necessary for cues to trigger cocaine seeking, whereas CVP (not RVP) is necessary for a cocaine prime to elicit reinstatement. Therefore, VP in general is critically involved in promoting relapse-related drug seeking, but its rostral vs. caudal aspects differentially mediate the motivational properties of previously learned cues vs. cocaine itself.

RVP-VTA Projection Specifically Mediates Cued Drug Seeking

To examine the wider neural circuits with which RVP and CVP interact to drive reinstatement, we focused on VP projections to VTA. First, we showed that RVP but not CVP projections to VTA are Fos-activated in proportion to cued reinstatement. To test whether these RVP efferents to VTA are also necessary for reinstatement, we induced hM4Di DREADD expression in RVP or CVP neurons, then microinjected the DREADD agonist CNO directly into VTA. This allowed us to specifically inhibit VP-VTA projections, but not other VP efferents.

When RVP projections to VTA (but not the adjacent SN) were inactivated in this manner, cue-induced reinstatement was abolished, but primed reinstatement was spared. In contrast, similar inhibition of CVP projections to VTA failed to affect either cued or primed reinstatement. Therefore, RVP projections to VTA are selectively recruited during cued reinstatement and are necessary for cues to trigger reinstatement, whereas CVP is necessary for a cocaine prime to promote reinstatement via VTA-independent circuitry.

RVP Indirectly Modulates Dopamine Neurons in Reinstatement—We identified a functional circuit containing RVP and VTA dopamine neurons (but not CVP, or SN dopamine neurons) that is necessary for cues to elicit reinstatement by functionally disconnecting RVP from VTA dopamine neurons via hM4Di inhibition of RVP in one hemisphere, and simultaneous hM4Di inhibition of VTA dopamine neurons in the contralateral hemisphere. This selective, bilateral circuit disruption reduced cue-induced reinstatement—indicating that serial connectivity between RVP and VTA dopamine neurons is required for cues to trigger cocaine seeking.

VP projections to VTA are predominantly GABAergic[3, 5, 32], and consistent with previous reports[32], we observed that DREADD-based inhibition of RVP inputs to VTA disinhibited dopamine neurons by decreasing sIPSC frequency. However, indiscriminate disinhibition of dopamine neurons is unlikely to account for attenuated reinstatement after we saw after RVP-VTA inactivation. When we directly disinhibited VTA dopamine neurons (as evidenced by robust Fos induction) with microinjections of the $GABA_A$ antagonist gabazine, cued reinstatement was instead *increased* (Fig. 7). It is therefore likely that reinstatement blockade by inhibition of RVP inputs to VTA involves differential modulation of heterogeneous VTA neuronal subpopulations, possibly including inhibition of non-dopaminergic VTA neurons. Interestingly, this modulation appears to be able to supersede

reinstatement-promoting effects of dopamine neuron disinhibition, which can also occur when the RVP-VTA circuit is inactivated. Systematic mapping of RVP inputs to VTA neuronal subpopulations will be required to further characterize the complexities of this novel, addiction-related circuit.

In addition to GABA efferents, RVP sends substantial Vglut2-containing projections to VTA [34]. However, DREADD-based inhibition of RVP-VTA projections did not reduce spontaneous excitatory transmission to TH+ cells, nor did a contralateral disconnect-based disruption of RVP glutamate projections to VTA affect cued reinstatement—arguing against a reinstatement-related glutamatergic RVP-VTA projection.

Conclusions

Here we showed that RVP projections to VTA are activated during, and are necessary for, cue-induced reinstatement, and that this requires modulation of VTA dopamine neurons. However, this modulation does not likely involve direct GABAergic or glutamatergic RVP projections onto dopamine neurons. Instead, inhibiting RVP inputs to VTA yielded both excitation of Type 1 VTA neurons, and inhibition of Type 2 neurons in vivo (Fig. 4). Type 1 neurons, which displayed conventionally dopaminergic electrophysiological characteristics, were excited by VP inhibition—consistent with our finding that inactivation of RVP inputs to VTA attenuates GABA inputs to TH+ neurons (Figure 4b–e). However, indiscriminate disinhibition of dopamine neurons with a $GABA_A$ antagonist did not impede reinstatement, but instead robustly facilitated it. Therefore, although our disconnection study revealed that dopamine neurons are needed for VP regulation of relapse, VP's role in reinstatement does not depend upon general disinhibition of dopamine neurons in VTA.

One possibility is that VP neurons selectively regulate a select subpopulation of VTA dopamine neurons during cued drug seeking. Notably, VTA contains fast-firing, thin-waveform dopamine neurons[46, 47], and it is possible that these could be the Type 2 neurons whose activity is suppressed after RVP-VTA inactivation (Fig. 4h–1). However, this seems unlikely because inhibitory inputs to dopamine neurons recorded in vitro here were nearly always reduced by DREADD-based inactivation of RVP-VTA projections (Fig. 4e). Therefore, we hypothesize that complex, subpopulation-specific VP modulation of VTA neurons is necessary for cues to elicit relapse to cocaine seeking. These findings call for additional research to characterize the relative connectivity of VP GABA, glutamate, acetylcholine, and peptide-containing neurons with VTA neuronal subpopulations, and to further define the roles for each in reward seeking.

In sum, we have described a novel pathway, the projection from RVP to VTA, which is necessary for conditioned drug seeking in a model of relapse in addiction. Furthermore, this circuit-behavior relationship requires RVP modulation of both non-dopamine and dopamine VTA neurons. We also showed that VP subregions play qualitatively different roles in drug seeking behavior elicited by either conditioned stimuli or drug itself. Together, these findings both expand the known circuitry of conditioned motivation[48], and also highlight important next directions for untangling the neural substrates of reward seeking behavior—especially in appetitive disorders such as drug addiction.

Online Methods

Subjects

159 male Sprague Dawley rats (250–350g; Charles River), and 45 outbred male Long Evans TH::Cre rats (hemizygous Cre+ n=35; Cre− littermates n=10)[33] were single or pair housed in a 12 h:12 h reverse light cycle vivarium (all tests conducted in dark period). No statistical methods were used to predetermine sample sizes, but they are similar to those reported in previous publications[15, 19, 23, 49]. All procedures were approved by MUSC's Institutional Animal Care and Use Committee.

Surgical Procedures

Animals were anesthetized with ketamine/xylazine/meloxicam (56.5/8.7/1.0 mg/kg), and implanted with indwelling jugular catheters. They received 20–30 nl injections of 0.5% CTb unilaterally in VTA, or 1 μl uni- or bilateral virus injections into RVP, CVP or VTA. VTA CTb and VP lentivirus injections were made by pneumatic pressure via a glass pipette (for CTb: 15–20 μm tip; for lentivirus: 30–45 μm tip) over 5 min and left in place 15–20 min. In TH::Cre animals, midbrain injections of an AAV floxed *DIO-Syn-hM4Di-mCherry* virus were made over 10 min through a Hamilton microinjection syringe. For bilateral VTA CNO or gabazine, or unilateral VTA glutamate antagonist or GABA agonist microinjections in behaving animals, guide cannulae were implanted 2 mm dorsal to VTA or SN.

Viral Constructs

hM4Di Inhibition of Ventral Pallidum—To transduce VP neurons with hM4Di DREADDs, we used a synapsin promoter-driven lentiviral vector with a GFP reporter, custom packaged (VSV-G envelope) by University of Pennsylvania vector core. To assist with identification, the hM4Di has an N-terminal hemagglutinin (HA) tag, and an IRES GFP reporter (S*yn-hM4Di-HA-GFP*; Fig. 1a). A *Syn-GFP* lentivirus (lacking the DREADD gene) was used to control for non-specific virus effects (Fig. 2b–c; Supplemental Fig. 5).

hM4Di Inhibition of Midbrain Dopamine Neurons—In TH::Cre transgenic rats[33], an AAV containing a double-floxed, inverted open reading frame hM4Di-mCherry sequence (*DIO-Syn-hM4Di-mCherry*; University of North Carolina Vector Core) was microinjected into ventral midbrain to express hM4Di receptors selectively in TH neurons of VTA or SN (Fig. 6a).

Localization of DREADD Expression

hM4Di receptor expression in cell bodies and processes was visualized with immunohistochemistry for HA, GFP, or mCherry tags (described below). Containment of transduction sites within RVP or CVP, or VTA or SN dopamine cells, was confirmed by co-staining for substance P (SP; defining borders of VP), or TH (defining VTA and SN), and a brain atlas[50]. A synapsin promoter virus was employed in VP, so some expression was observed outside the borders of RVP or CVP in most animals. Animals with more than 30% of DREADD expression observed outside RVP or CVP were excluded from analyses (n=7). For animals with RVP virus injections, no more than 20% of DREADD-expressing tissue encroached into CVP (i.e., caudal of bregma), or vice versa. Animals injected with the *Syn-*

GFP control virus in VP had comparable GFP expression patterns to hM4Di animals. For TH::Cre rats, hM4Di expression was robust in either VTA or SN, and was restricted almost exclusively to TH+ cell bodies and processes [% mCherry+ neurons coexpressing TH: m ±SEM=97.5±0.7%; Fig. 6b–c, Supplemental Fig. 6]. mCherry expression was not observed in the contralateral hemisphere, nor did expression extend substantially into the SN of VTA-injected animals, or into VTA of SN-injected animals (Fig. 6b–c).

Electrophysiological Validation of DREADD-Based Inhibition of VP Neurons and Efferents

In Vitro Electrophysiology in Brain Slices—Brain slices from VP S*yn-hM4Di-HA-GFP* (n=6 rats), and *Syn-GFP* animals (n=2) were prepared as previously described[49]. Slice physiology data collection and analysis was not performed blind to the experimental group. Horizontal sections containing VTA were transferred to a 32–34°C chamber containing a carbogen-bubbled aCSF solution.

Slices were transferred to a recording chamber and perfused with 32°C aCSF at 2 ml/min. Neurons were visually identified under infrared light using Dodt gradient contrast imaging. Recording pipettes with a resistance of 1–3 MΩ were filled with internal solution containing: (in mM): CsCl (120), HEPES (10), $MgCl_2$ (2), EGTA (1), Na_2ATP (2), NaGTP (0.3), 0.2% biocytin; 295 mOsm, pH = 7.3. To isolate sIPSCs, recording aCSF was supplemented with AMPA/NMDA antagonists (NBQX/AP5; 10 μM/100 μM; Abcam), and for sEPSC recordings, picrotoxin (100 μM; Tocris) was added to ACSF. Neurons medial to the nucleus of the accessory optic tract were targeted for patch clamp (in the vicinity of dense, GFP-expressing RVP afferents), and whole-cell mode was achieved while holding the cell at -−70mV.

Data were acquired using an Axon MultiClamp 700B amplifier and an ITC-18 digital interface (HEKA Instruments) controlled by AxographX software. Recordings were filtered at 4 kHZ and acquired at 10 kHz, and sIPSCs were detected and analyzed using the template-matching event-detection algorithm in AxographX. Detection parameters were set at amplitude >4 pA, and acquired events were visually inspected before averaging. We recorded at least 150 spontaneous currents during a baseline period, and following 10 min of 5 μM CNO perfusion. Series resistance (R_s) was monitored throughout the recording and an experiment was discontinued if R_s exceeded 25 MΩ or changed more than 25%.

In vivo electrophysiology—In vivo electrophysiology data collection and analysis were performed blind to experimental conditions. Glass recording pipettes (5–12 MΩ) were filled with 2% pontamine sky blue in 0.5 M sodium acetate. A glass injection pipette (20 μm tip) glued ~150 μm behind the recording tip delivered 60 nl of 100 μM CNO to VP or VTA neurons via brief pneumatic pulses. Multiple CNO applications occurred in each animal upon different cells, each separated by >30 min. Signals were amplified and filtered (0.3–5 kHz) using a Model 1600 Neuroprobe Amplifier (A-M Systems) and a BMA 200 Bioamplifier (CWE), before digital conversion and recording to Spike 2 (v5.21) via a Micro 1401 MkII interface (CED). Body temperature was maintained at 36.0–37.5°C throughout recording.

Recorded VP neurons were located nearby prior virus injections, and identified by their firing rates and waveforms, as previously reported[12]. For confirmation of recording locations, markings 1 mm above and immediately below recording tracks in each VP and VTA site were made by iontophoretic dye deposits immediately prior to perfusion. VTA "Type 1" neurons were identified by electrophysiological criteria traditionally describing dopamine neurons[26], including (1) biphasic or triphasic waveform >2.5 ms in duration, (2) >1.1 ms from spike onset to negative trough, and (3) spontaneous firing rate <10 Hz. All cells included in analyses were from confirmed recordings in VP or VTA.

Drugs and Tract Tracers

Cocaine HCl (NIDA) was dissolved in 0.9% sterile saline. CTb (Sigma) was dissolved at 0.5% in 0.1 M PBS. CNO was obtained from the NIH RAID program (Jürgen Wess; NIDDK). For systemic administration, CNO (0, 0.1, 1, 10 & 20 mg/kg) was dissolved in 5% DMSO, then diluted to a 1 ml/kg volume with 0.9% saline. For intracranial administration, CNO was dissolved in aCSF to 100 μM (in vivo electrophysiology) or 1 mM (behavioral microinjection), or 5 μM in vitro. Gabazine (10&100 μM), baclofen/muscimol (0.3/0.03 mM), and CNQX/AP5 (0.7/1.6 mM; all from Sigma) were dissolved in aCSF for 0.3 μl VTA microinjections.

Behavioral Training and Testing Procedures

Behavioral training and testing took place in standard Med Associates operant chambers described elsewhere[23]. Rats underwent 10 daily 2 h self-administration sessions (>10 cocaine infusions/day, 0.2 mg/50 μl infusion). Pressing one lever yielded a 3.6 s cocaine infusion, tone, and light above the active lever (FR1 schedule), followed by a 20 s timeout, when pressing was recorded but did not yield cocaine or cues (Figure 2a). Inactive lever presses were recorded, but had no consequences. Animals then received 7+ d of extinction training (until criterion: <25 presses for 2 consecutive days), where lever presses yielded neither cocaine nor cues.

During 2 h cue-induced reinstatement tests, active lever presses yielded cocaine cues, but no cocaine. For cocaine priming tests, 10 mg/kg *i.p.* cocaine was administered immediately prior to the 2 h test, where lever presses yielded neither cocaine nor cues. For the CTb/Fos experiment, animals were perfused immediately after one of the following 2 h test sessions: CS+ reinstatement, an additional extinction session, exposure to a novel environment, or exposure to a discrete CS− (details in[23]). Behavior during the first 30 min of tests (which most influences Fos protein measured 90 min later) was compared to neuronal activation (Fig. 3).

Animals that received systemic CNO had 3 cued, and 3 cocaine primed reinstatement tests each. 30 min prior to each test, RVP (n=16) or CVP (n=17) S*yn-hM4Di-HA-GFP* animals, VP *Syn-GFP* animals (n=5), and animals with no virus expression (n=9) received counterbalanced *i.p.* injections of vehicle, and 2 doses of CNO [0.1 mg/kg: n=25; 1.0 mg/kg: n=25; 10 mg/kg: n=26; 20 mg/kg: n=30). Other animals received counterbalanced intra-VTA (after RVP or CVP S*yn-hM4Di-HA-GFP*) or intra-SN (after RVP S*yn-hM4Di-HA-GFP*) microinjections of vehicle (aCSF) and CNO (1 mM/0.3 μl) 5 min prior to each of 2

cued, and 2 primed reinstatement tests. Some of these animals were later habituated to an open field for 2 d, then locomotor activity after vehicle and CNO was tested over 2 d, 48 h+ apart (intra-VTA CNO: 0&1 mM/0.3 μl, n=23). TH::Cre animals (RVP S*yn-hM4Di-HA-GFP* +VTA *DIO-Syn-hM4Di-mCherry*: Cre+ n=9, Cre- n=10; RVP S*yn-hM4Di-HA-GFP* +SN *DIO-Syn-hM4Di-mCherry*: Cre+ n=8; VTA *DIO-Syn-hM4Di-mCherry* only n=6) received *i.p*. vehicle or CNO (10 mg/kg) 30 min before each of two cue-induced reinstatement tests. Animals with unilateral RVP S*yn-hM4Di-HA-GFP* +contralateral VTA cannulae underwent 3 cued reinstatement tests after unilateral VTA vehicle+*i.p.* CNO (10 mg/kg), and two of the following: intra-VTA baclofen/muscimol+ *i.p.* CNO (n=12 rats), intra-VTA CNQX/AP5+ *i.p.* CNO (n=5), intra-VTA baclofen/muscimol+ *i.p.* vehicle (n=8). For bilateral VTA gabazine, animals also underwent 2–3 reinstatement tests, after vehicle and 10 μM (n=7 rats), and 100 μM (n=4) gabazine (high dose testing was discontinued due to intense nonspecific locomotor activation). Vehicle/CNO injection order was counterbalanced in all cases.

Tissue Preparation and Staining

Animals were deeply anesthetized and perfused with 0.9% saline, followed by 4% paraformaldehyde. Brains were postfixed in 4% paraformaldehyde, cryoprotected, and sliced at 30–40 μm on a cryostat. For CTb/Fos staining, IHC procedures were described previously[23]. To visualize hM4Di expression, we performed immunohistochemistry for HA, mCherry, and/or GFP tags. VP borders were defined via immunoreactivity for SP[4], and dopamine cells were identified as TH immunoreactive. All tissue was first incubated in 3% normal donkey serum PBS-Triton (PBST; 2 h), then in primary antibodies in PBST overnight at RT. The following primary antibodies were used in these experiments (1 or 2 antibodies/tissue sample): mouse anti HA (1:500; Covance catalogue number: MMS-101P), rabbit anti DsRed (mCherry tag; 1:500; Clontech catalogue number: 632496), chicken anti GFP (1:2000; Abcam catalogue number: ab13970), rabbit anti SP (1:5000; Immunostar catalogue number: 20064), and mouse anti TH (1:1000, Immunostar catalogue number: 22941). For fluorescent stains, sections were incubated 4 h at RT in fluorescent conjugated secondary antibodies [donkey anti mouse 488 (HA and TH: 1:500; Invitrogen catalogue number: A21202), donkey anti rabbit 594 (Ds Red, TH, and SP: 1:500; Invitrogen catalogue number: A21207), donkey anti chicken 488 (GFP, Fos: 1:500, Jackson catalogue number: 703545155)]. Slices were mounted and coverslipped with Citifluor mounting medium. For DAB visualization of HA, slices were incubated 2 h in a biotinylated donkey anti mouse secondary antibody (1:500; Jackson catalogue number: 715066151), and amplified with an avidin-biotin complex (1:500; Vector). Tissue was dehydrated and coverslipped with Permount. After slice physiology experiments, tissue was fixed 48h in 4% paraformaldehyde, sectioned, incubated in 5% normal goat serum PBST (7min), rabbit anti TH (1:1000; Millipore catalogue number: AB152) and Avidin TexasRed (1:500; Life Technologies catalogue number: A820) overnight at 4°C, and Alexafluor 488 goat anti-rabbit IgG (Life Technologies catalogue number: A11008) for 2h. All antibodies were previously validated for specificity, as described on the manufacturer's websites and the *Journal of Comparative Neurology* antibody database.

Quantification of CTb/Fos staining

Fos expression in CTb+ cells was analyzed as a function of rostral/caudal position within VP, using a quantification strategy described in a previous report, where other analyses of this tissue were described[23]. Coronal sections at ~250 μm intervals throughout the rostral/caudal extent of VP were photographed at 10X magnification, and montaged with the Stereo Investigator Virtual Slice Module (MBF Bioscience) to preserve anatomical landmarks. All CTb+ neurons (with or without Fos) within VP ipsilateral to VTA CTb injection were counted on each slice by an observer blind to experimental group, and primary analyses examined the percentage of total CTb neurons that were Fos+ (Fig. 3, Supplemental Fig. 2), or average number of CTb cells per rostro-caudal level (Supplemental Fig. 3). To quantify VTA gabazine (vehicle or 10 μM)-induced Fos, z-stack images were taken at 20X magnification of TH (red) and Fos (green) immunoreactivity, 90–110 μm lateral of VTA microinjection sites (Fig. 7). TH+ and Fos+ neurons were quantified in Photoshop using ImageJ-deconvolved images. 2–3 images/microinjection were quantified and averaged for each animal.

Analysis and Statistics

To examine reinstatement-related Fos expression in VTA-projecting neurons within RVP and CVP, total CTb+, and CTb+/Fos+, cells in VP (ipsilateral of VTA CTb injections) were quantified at ~250 μm intervals in each animal. One-way ANOVA (with Tukey posthoc comparisons) were used to analyze percentages of Fos+ CTb neurons between behavioral groups. Average percentages of Fos+ CTb neurons in RVP (rostral of bregma) or CVP (caudal of bregma) for each animal were also correlated with active lever pressing in the first 30 min of cued reinstatement, 90 min before sacrifice (Pearson's test). For gabazine-induced Fos in VTA, average TH+, and TH+/Fos+ neurons were computed for each animal after bilateral vehicle (n=3 rats) or gabazine (n=5), and compared with between-subjects t-tests.

Effects of systemic CNO on cued or primed reinstatement were analyzed with mixed ANOVAs for CNO dose (between subjects variable) X lever (active or inactive; within subjects) for each behavioral group (RVP S*yn-hM4Di-HA-GFP*, CVP S*yn-hM4Di-HA-GFP; Syn-GFP*, or no virus). Repeated measures drug X lever ANOVAs tested effects of CNO in VTA or SN on cued or primed reinstatement in RVP or CVP S*yn-hM4Di-HA-GFP* animals, and systemic CNO on cued reinstatement in TH::Cre rats. One way ANOVAs were used to test effects of bilateral VTA gabazine, and contralaterally disconnecting RVP from VTA, or VTA glutamate, on cued reinstatement. Tukey or Bonferroni-corrected t-test posthoc analyses were used as appropriate to determine the nature of significant main effects and interactions. All tests were two-tailed, and normality of data distribution was tested with Mauchly's test of Sphericity (Greenhouse-Geisser corrected if necessary).

For in vitro electrophysiology, the change in firing rate of VP or VTA neurons was determined from 100 s epochs immediately before vs during CNO application with paired samples t-tests comparing average pre- vs. post- CNO sIPSC or sEPSC amplitude or frequency, and 2-way ANOVAs with Bonferroni posthocs. Results were normalized to pre-CNO firing rate (100%) for each cell. In vivo, two-tailed t-tests or Wilcoxon signed-rank

paired sample tests were used to compare pre- and post-CNO firing rates in VP and VTA (depending on normality computed by D'Agostino-Pearson omnibus test). Silenced neurons were included in analyses if the original waveform returned within 200 s post-CNO application. Baseline firing rates of VP neurons were compared using a two-tailed unpaired t-test with Welch's correction due to a significant F-test for unequal variance.

Supplementary Material

Refer to Web version on PubMed Central for supplementary material.

Acknowledgments

We thank Phong Do, Meghin J. Gilstrap, and Edwin C. Lin for assistance with behavioral testing and immunohistochemistry, and Bryan L. Roth for DREADD constructs and consultation on DREADDs. Clozapine-n-oxide was obtained from the NIH as part of the Rapid Access to Investigative Drug Program funded by the NINDS. Research was supported by NIH grants: F32 DA026692, K99 DA035251 (SVM), F31 DA030891 (JTB), R21 DA025837 (GA-J & SPW), R01 DA013951 (JJW), R37 DA006214, P50 DA015369 (GA-J). This project was supported by the National Center for Research Resources and the Office of the Director of the National Institutes of Health through Grant Number C06 RR015455.

References

1. Zahm DS, Heimer L. Two transpallidal pathways originating in the rat nucleus accumbens. J Comp Neurol. 1990; 302:437–446. [PubMed: 1702109]
2. Zahm DS, Williams E, Wohltmann C. Ventral striatopallidothalamic projection: IV. Relative involvements of neurochemically distinct subterritories in the ventral pallidum and adjacent parts of the rostroventral forebrain. J Comp Neurol. 1996; 364:340–362. [PubMed: 8788254]
3. Kalivas PW, Churchill L, Klitenick MA. GABA and enkephalin projection from the nucleus accumbens and ventral pallidum to the ventral tegmental area. Neuroscience. 1993; 57:1047–1060. [PubMed: 7508582]
4. Haber SN, Nauta WJ. Ramifications of the globus pallidus in the rat as indicated by patterns of immunohistochemistry. Neuroscience. 1983; 9:245–260. [PubMed: 6192358]
5. Floresco SB, West AR, Ash B, Moore H, Grace AA. Afferent modulation of dopamine neuron firing differentially regulates tonic and phasic dopamine transmission. Nat Neurosci. 2003; 6:968–973. [PubMed: 12897785]
6. Smith KS, Tindell AJ, Aldridge JW, Berridge KC. Ventral pallidum roles in reward and motivation. Behavioural brain research. 2009; 196:155–167. [PubMed: 18955088]
7. Mogenson, GJ.; Brudzynski, SM.; Wu, M.; Yang, CY.; Yim, CY. From motivation to action: A review of dopaminergic regulation of limbic to nucleus accumbens to ventral pallidum to pedunculopontine nucleus circuitries involved in limbic-motor integration. In: Kalivas, PW.; Barnes, CD., editors. Limbic Motor Circuits in Neuropsychiatry. CRC Press; Boca Raton, FL: 1993. p. 193-236.
8. Churchill L, Kalivas PW. A topographically organized gamma-aminobutyric acid projection from the ventral pallidum to the nucleus accumbens in the rat. J Comp Neurol. 1994; 345:579–595. [PubMed: 7962701]
9. Heimer L, Zahm DS, Churchill L, Kalivas PW, Wohltmann C. Specificity in the projection patterns of accumbal core and shell in the rat. Neuroscience. 1991; 41:89–125. [PubMed: 2057066]
10. Kupchik YM, Kalivas PW. The rostral subcommissural ventral pallidum is a mix of ventral pallidal neurons and neurons from adjacent areas: an electrophysiological study. Brain Struct Funct. 2012
11. Root DH, et al. Differential roles of ventral pallidum subregions during cocaine self-administration behaviors. J Comp Neurol. 2013; 521:558–588. [PubMed: 22806483]
12. Yang CR, Mogenson GJ. Ventral pallidal neuronal responses to dopamine receptor stimulation in the nucleus accumbens. Brain Res. 1989; 489:237–246. [PubMed: 2568154]

13. McBride WJ, Murphy JM, Ikemoto S. Localization of brain reinforcement mechanisms: intracranial self-administration and intracranial place-conditioning studies. Behav Brain Res. 1999; 101:129–152. [PubMed: 10372570]
14. Panagis G, Miliaressis E, Anagnostakis Y, Spyraki C. Ventral pallidum self-stimulation: a moveable electrode mapping study. Behav Brain Res. 1995; 68:165–172. [PubMed: 7654303]
15. Bengtson CP, Osborne PB. Electrophysiological properties of cholinergic and noncholinergic neurons in the ventral pallidal region of the nucleus basalis in rat brain slices. J Neurophysiol. 2000; 83:2649–2660. [PubMed: 10805665]
16. Zahm DS, Heimer L. Ventral striatopallidal parts of the basal ganglia in the rat: I. Neurochemical compartmentation as reflected by the distributions of neurotensin and substance P immunoreactivity. J Comp Neurol. 1988; 272:516–535. [PubMed: 2458391]
17. Johnson PI, Stellar JR, Paul AD. Regional reward differences within the ventral pallidum are revealed by microinjections of a mu opiate receptor agonist. Neuropharmacology. 1993; 32:1305–1314. [PubMed: 8152522]
18. Calder AJ, et al. Disgust sensitivity predicts the insula and pallidal response to pictures of disgusting foods. Eur J Neurosci. 2007; 25:3422–3428. [PubMed: 17553011]
19. Smith KS, Berridge KC. The ventral pallidum and hedonic reward: neurochemical maps of sucrose “liking” and food intake. The Journal of neuroscience : the official journal of the Society for Neuroscience. 2005; 25:8637–8649. [PubMed: 16177031]
20. Grace AA, Floresco SB, Goto Y, Lodge DJ. Regulation of firing of dopaminergic neurons and control of goal-directed behaviors. Trends Neurosci. 2007; 30:220–227. [PubMed: 17400299]
21. Tindell AJ, Berridge KC, Aldridge JW. Ventral pallidal representation of pavlovian cues and reward: population and rate codes. J Neurosci. 2004; 24:1058–1069. [PubMed: 14762124]
22. Tachibana Y, Hikosaka O. The primate ventral pallidum encodes expected reward value and regulates motor action. Neuron. 2012; 76:826–837. [PubMed: 23177966]
23. Mahler SV, Aston-Jones GS. Fos activation of selective afferents to ventral tegmental area during cue-induced reinstatement of cocaine seeking in rats. J Neurosci. 2012; 32:13309–13326. [PubMed: 22993446]
24. Armbruster BN, Li X, Pausch MH, Herlitze S, Roth BL. Evolving the lock to fit the key to create a family of G protein-coupled receptors potently activated by an inert ligand. Proc Natl Acad Sci U S A. 2007; 104:5163–5168. [PubMed: 17360345]
25. Ferguson SM, Neumaier JF. Grateful DREADDs: engineered receptors reveal how neural circuits regulate behavior. Neuropsychopharmacology. 2012; 37:296–297. [PubMed: 22157861]
26. Ungless MA, Grace AA. Are you or aren’t you? Challenges associated with physiologically identifying dopamine neurons. Trends Neurosci. 2012
27. Ikemoto S. Dopamine reward circuitry: two projection systems from the ventral midbrain to the nucleus accumbens-olfactory tubercle complex. Brain Res Rev. 2007; 56:27–78. [PubMed: 17574681]
28. Morales M, Pickel VM. Insights to drug addiction derived from ultrastructural views of the mesocorticolimbic system. Ann N Y Acad Sci. 2012; 1248:71–88. [PubMed: 22171551]
29. Fields HL, Hjelmstad GO, Margolis EB, Nicola SM. Ventral tegmental area neurons in learned appetitive behavior and positive reinforcement. Annu Rev Neurosci. 2007; 30:289–316. [PubMed: 17376009]
30. van Zessen R, Phillips JL, Budygin EA, Stuber GD. Activation of VTA GABA neurons disrupts reward consumption. Neuron. 2012; 73:1184–1194. [PubMed: 22445345]
31. Stamatakis AM, et al. A unique population of ventral tegmental area neurons inhibits the lateral habenula to promote reward. Neuron. 2013; 80:1039–1053. [PubMed: 24267654]
32. Hjelmstad GO, Xia Y, Margolis EB, Fields HL. Opioid modulation of ventral pallidal afferents to ventral tegmental area neurons. J Neurosci. 2013; 33:6454–6459. [PubMed: 23575843]
33. Witten IB, et al. Recombinase-driver rat lines: tools, techniques, and optogenetic application to dopamine-mediated reinforcement. Neuron. 2011; 72:721–733. [PubMed: 22153370]
34. Geisler S, Derst C, Veh RW, Zahm DS. Glutamatergic afferents of the ventral tegmental area in the rat. J Neurosci. 2007; 27:5730–5743. [PubMed: 17522317]

35. McFarland K, Kalivas PW. The circuitry mediating cocaine-induced reinstatement of drug-seeking behavior. J Neurosci. 2001; 21:8655–8663. [PubMed: 11606653]
36. McFarland K, Davidge SB, Lapish CC, Kalivas PW. Limbic and motor circuitry underlying footshock-induced reinstatement of cocaine-seeking behavior. J Neurosci. 2004; 24:1551–1560. [PubMed: 14973230]
37. Robledo P, Koob GF. Two discrete nucleus accumbens projection areas differentially mediate cocaine self-administration in the rat. Behav Brain Res. 1993; 55:159–166. [PubMed: 8395179]
38. Farrar AM, et al. Forebrain circuitry involved in effort-related choice: Injections of the GABAA agonist muscimol into ventral pallidum alter response allocation in food-seeking behavior. Neuroscience. 2008; 152:321–330. [PubMed: 18272291]
39. Colussi-Mas J, Geisler S, Zimmer L, Zahm DS, Berod A. Activation of afferents to the ventral tegmental area in response to acute amphetamine: a double-labelling study. Eur J Neurosci. 2007; 26:1011–1025. [PubMed: 17714194]
40. Geisler S, et al. Prominent activation of brainstem and pallidal afferents of the ventral tegmental area by cocaine. Neuropsychopharmacology. 2008; 33:2688–2700. [PubMed: 18094667]
41. Childress AR, et al. Prelude to passion: limbic activation by “unseen” drug and sexual cues. PLoS ONE. 2008; 3:e1506. [PubMed: 18231593]
42. Zahm DS. Is the caudomedial shell of the nucleus accumbens part of the extended amygdala? A consideration of connections. Critical reviews in neurobiology. 1998; 12:245–265. [PubMed: 9847057]
43. Tripathi A, Prensa L, Mengual E. Axonal branching patterns of ventral pallidal neurons in the rat. Brain Struct Funct. 2012
44. Leung BK, Balleine BW. The ventral striato-pallidal pathway mediates the effect of predictive learning on choice between goal-directed actions. J Neurosci. 2013; 33:13848–13860. [PubMed: 23966704]
45. Robinson MJ, Berridge KC. Instant transformation of learned repulsion into motivational “wanting”. Current biology : CB. 2013; 23:282–289. [PubMed: 23375893]
46. Lammel S, et al. Unique properties of mesoprefrontal neurons within a dual mesocorticolimbic dopamine system. Neuron. 2008; 57:760–773. [PubMed: 18341995]
47. Luo AH, Georges FE, Aston-Jones GS. Novel neurons in ventral tegmental area fire selectively during the active phase of the diurnal cycle. Eur J Neurosci. 2008; 27:408–422. [PubMed: 18215237]
48. Robinson TE, Berridge KC. Addiction. Annu Rev Psychol. 2003; 54:25–53. [PubMed: 12185211]
49. Beckley JT, Evins CE, Fedarovich H, Gilstrap MJ, Woodward JJ. Medial prefrontal cortex inversely regulates toluene-induced changes in markers of synaptic plasticity of mesolimbic dopamine neurons. J Neurosci. 2013; 33:804–813. [PubMed: 23303956]
50. Paxinos, G.; Watson, C. The rat brain in stereotaxic coordinates. Academic Press/Elsevier; Amsterdam ; Boston: 2006.

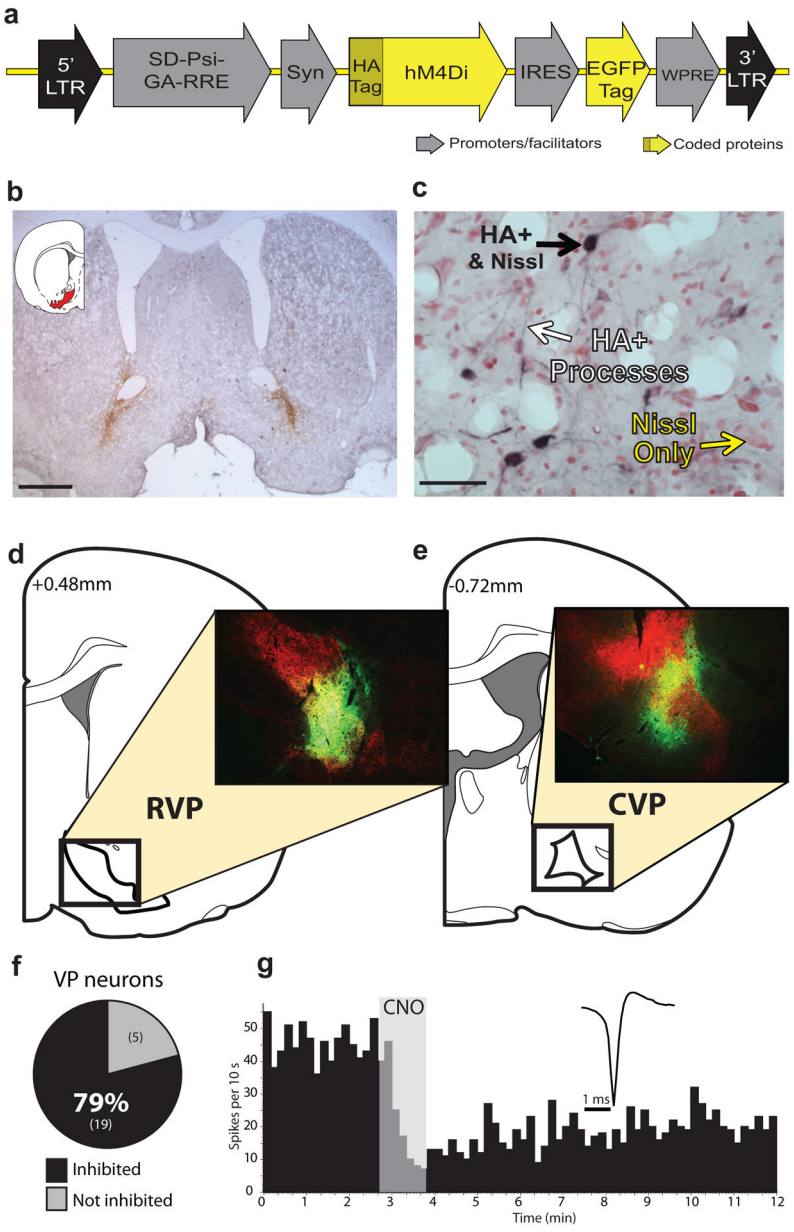

Figure 1. hM4Di inhibitory DREADD expression and function

a) S*yn-hM4Di-HA-GFP* lentivirus used to express hM4Di DREADDs under a neuronal-specific human synapsin promoter (*Syn*) in RVP or CVP. **b)** Typical staining for HA-tagged hM4Di after bilateral injections into RVP. Scale bar=1 mm. **c)** HA-tagged hM4Di receptors are expressed on cell bodies and processes (black staining) in VP (neutral red counterstain). Scale bar=50 μm. **d)** Typical HA expression (green) in RVP, largely contained within VP borders (defined with SP counterstain in red). **e)** Typical HA expression in CVP, largely contained within VP borders (as defined in d). Images in b–e are representative of DREADD expression seen in experimental groups, ns listed in Results. **f)** In animals with S*yn-hM4Di-HA-GFP* in RVP or CVP, local application of 100 μM CNO onto extracellularly recorded VP neurons in vivo (via double barrel glass pipette) inhibited firing rates in the vast majority

of neurons tested (19/24). **g)** Typical change in discharge rate of a VP neuron (waveform inset) after local CNO application (shaded region).

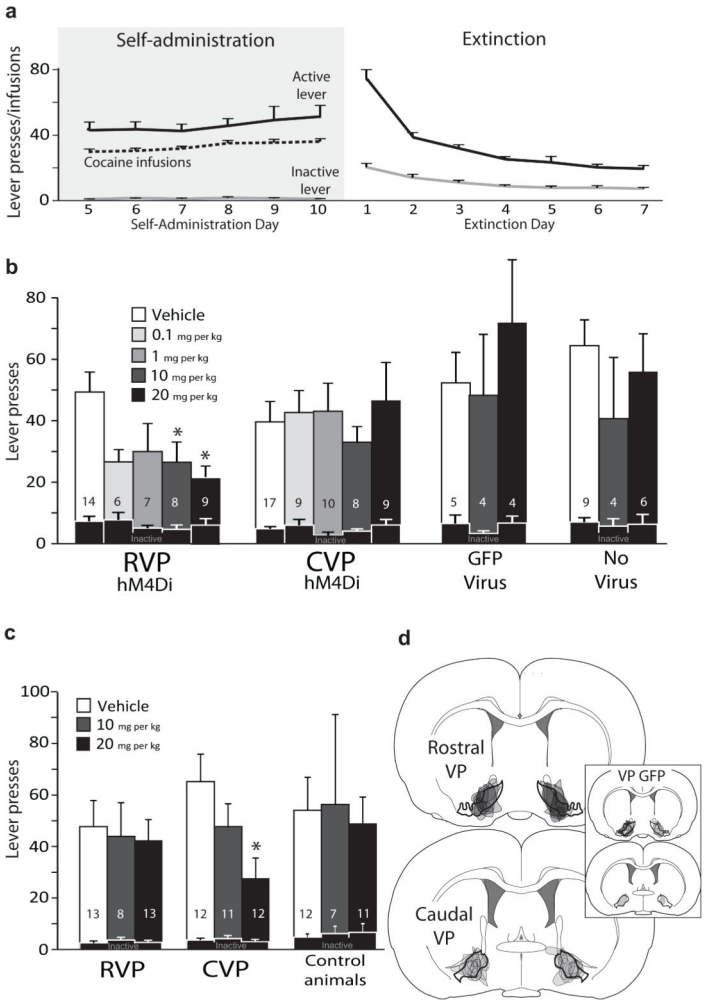

Figure 2. Effects of inactivating rostral or caudal VP on reinstatement of cocaine seeking

a) Daily m±SEM cocaine infusions and active/inactive lever presses for the last 6 days of criterion self- administration (>10 infusions/day), and active/inactive lever presses for the first 7 days of extinction training. **b)** Active lever presses during cue-induced reinstatement following different doses of the DREADD agonist clozapine-n-oxide (CNO; dose=bar color; vehicle, 0.1, 1, 10, 20 mg/kg), in animals with bilateral RVP or CVP S*yn-hM4Di-HA-GFP* virus, bilateral VP control virus (*Syn-GFP)*, or no virus expression. Inactive lever presses during reinstatement are shown with overlaid black bars. *****Vehicle vs. 10 mg/kg CNO: p=0.001, vehicle vs. 20 mg/kg CNO: p=0.015. **c)** Active and inactive lever presses during cocaine primed reinstatement following different doses of CNO (Vehicle, 10, 20 mg/kg), in animals with RVP or CVP S*yn-hM4Di-HA-GFP* virus, or controls (*Syn-GFP* or no virus expression animals). *****Vehicle vs. 20 mg/kg CNO: p=0.008. Bars and lines=m±SEM. **d)** The anatomical localization of virus expression sites (as visualized with HA or GFP immunoreactivity) is represented for animals injected with S*yn-hM4Di-HA-GFP* in RVP (black) or CVP (grey), or *Syn-GFP* (grey; inset).

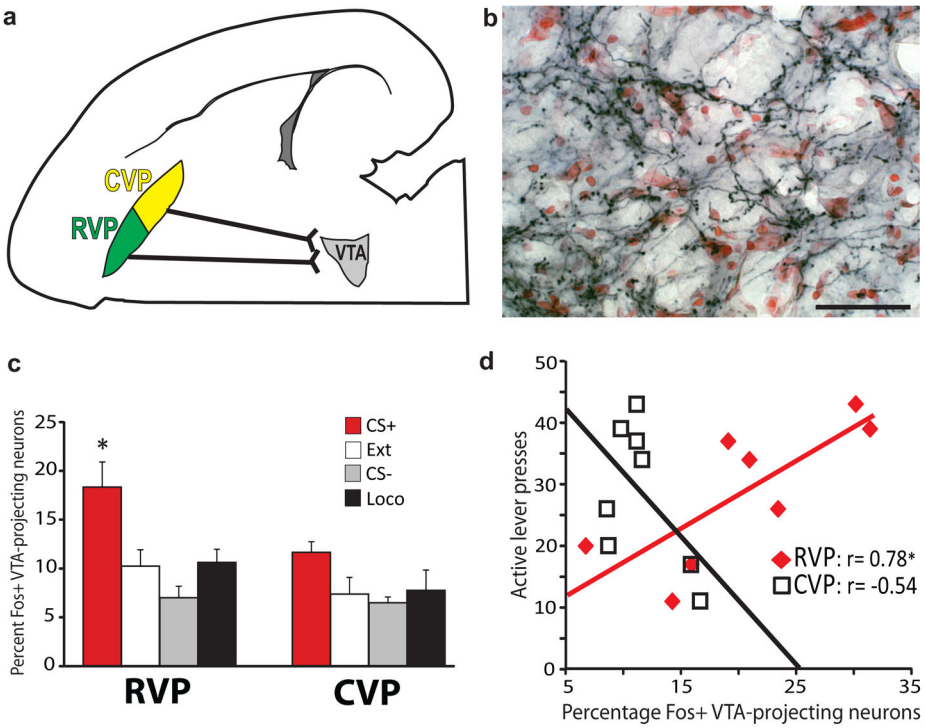

Figure 3. Rostral VP projections to VTA are Fos-activated during cued reinstatement

a) Predominantly ipsilateral projections from RVP and CVP to VTA are diagrammed in the horizontal plane. **b)** Axon terminals in VTA express the anterogradely-transported, HA-tagged hM4Di receptor (black axonal processes) after S*yn-hM4Di-HA-GFP* injection in ipsilateral RVP (red Nissl counterstain in VTA). Coronal view, scale bar=50 μm. Image is representative of VP axonal DREADD expression in VTA of experimental animals, group ns listed in Results. **c)** Mean±SEM percentages of VTA-projecting (CTb+) RVP or CVP cells that express Fos after cue-induced reinstatement (CS+), or control behavioral conditions, where animals were exposed to: the extinguished self-administration environment without cues or cocaine (Ext), a tone/light stimulus not associated with cocaine (CS−), or a locomotion- enhancing novel environment (Loco). A greater proportion of VTA-projecting neurons in RVP were Fos-activated in CS+ than in control animals [*****CS+ different from: Ext (p=0.01), CS− (p=0.005), and Loco (p=0.025)]. No significant behavior-specific activation of VTA-projecting neurons was detected in CVP. Bars=m±SEM. **d)** Cue-induced reinstatement behavior was positively correlated with Fos activation of VTA-projecting neurons in RVP (*Pearson correlation: p=0.02), but not CVP (not significant).

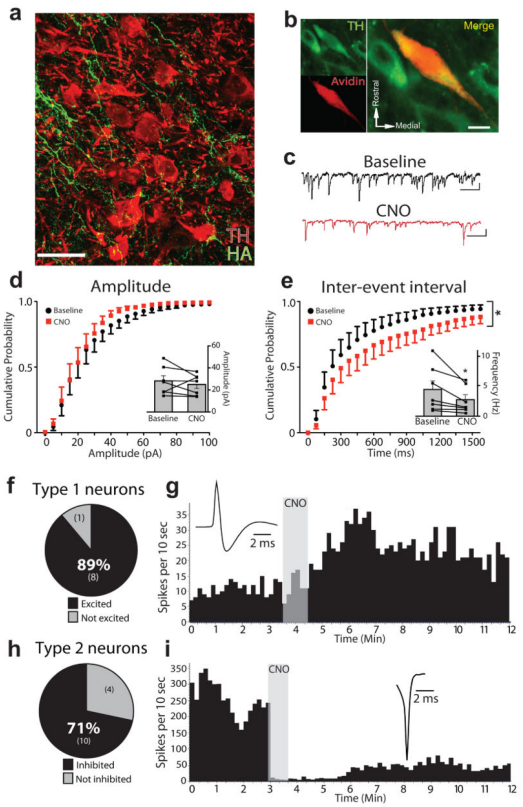

Figure 4. Inactivating rostral VP afferents modulates VTA cell firing

a) hM4Di receptors (green) are expressed on RVP axon terminals in the vicinity of TH-labeled dopamine neurons (red) in VTA. Scale bar=30 μm. Image is representative of VP axonal DREADD expression in VTA of experimental animals, ns listed in Online Methods. **b)** In slice electrophysiology experiments, recorded neurons were filled with biotin, labeled with avidin (red), and identified as dopaminergic by co-labeling for TH (green). Scale bar=10 μm. **c)** Representative traces from VTA dopamine neurons are shown in baseline conditions (top, black), and after CNO (bottom, red; scale=20 pA, 200 ms). **d)** CNO had no effect on the cumulative distribution or mean (inset) sIPSC amplitude. Points=m±SEM, Lines in inset=individual raw values. **e)** CNO shifted the inter-event interval cumulative distribution to the right (*baseline vs. CNO, p=0.0002) and decreased mean sIPSC frequency (Inset, *baseline vs. CNO, p=0.046). Points=m±SEM, lines in inset=individual raw values. **f)** In vivo, 8/9 putatively dopaminergic “Type 1” neurons in VTA were excited by local application of CNO in the vicinity of hM4Di-expressing RVP terminals in VTA. **g)** Rate histogram demonstrating effect of local CNO application in vivo (60 nl; shaded region) on firing of a “Type 1” neuron (waveform inset) in VTA of RVP-hM4Di animal. **h)** 10/14 fast-firing, short-waveform “Type 2” neurons were inhibited by local application of CNO in vivo, in the vicinity of hM4Di-expressing RVP terminals in VTA. **i)** Example change in discharge rate of “Type 2” neuron (waveform inset) in VTA after local CNO application in vivo (60 nl; shaded region) in a RVP- hM4Di animal.

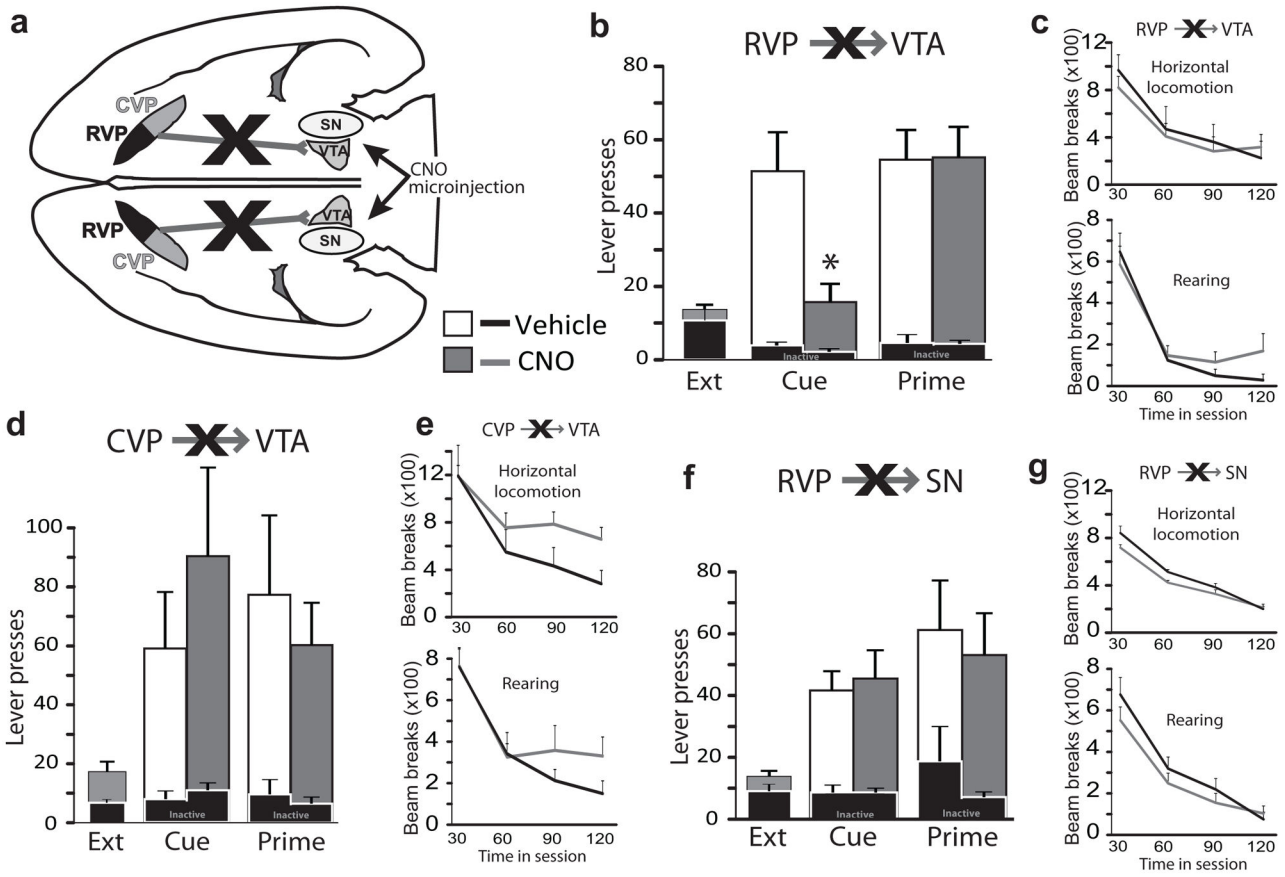

Figure 5. Inactivating rostral VP projection to VTA blocks cued reinstatement

a) Projections from RVP to VTA or SN, or from CVP to VTA, were transiently inactivated by local midbrain microinjection of CNO amongst VP axon terminals expressing hM4Di receptors. **b)** Inactivation of VTA terminals from RVP blocked cue-induced (Cue), but not cocaine primed (Prime) reinstatement of cocaine seeking. Active lever pressing during the last day of extinction training (Ext., bars at left), and reinstatement after VTA vehicle (white bars) or VTA CNO (grey bars) are shown. Inactive lever presses are represented with black bars at bottom. ***** $p<0.001$. **c)** Inactivating RVP projections to VTA did not affect horizontal (top graph) or vertical (rearing; bottom graph) locomotion in a familiar environment. Locomotion (beam breaks) during 30 min bins in the 2 h session is shown after VTA microinjection of vehicle (black lines) or CNO (grey lines). **d, e)** Inactivation of CVP efferents to VTA did not affect cue-induced or cocaine-primed reinstatement, nor did it significantly affect horizontal locomotion or rearing. **f, g)** Inactivation of RVP projections to SN failed to affect reinstatement or locomotor behavior. Bars and lines=m±SEM.

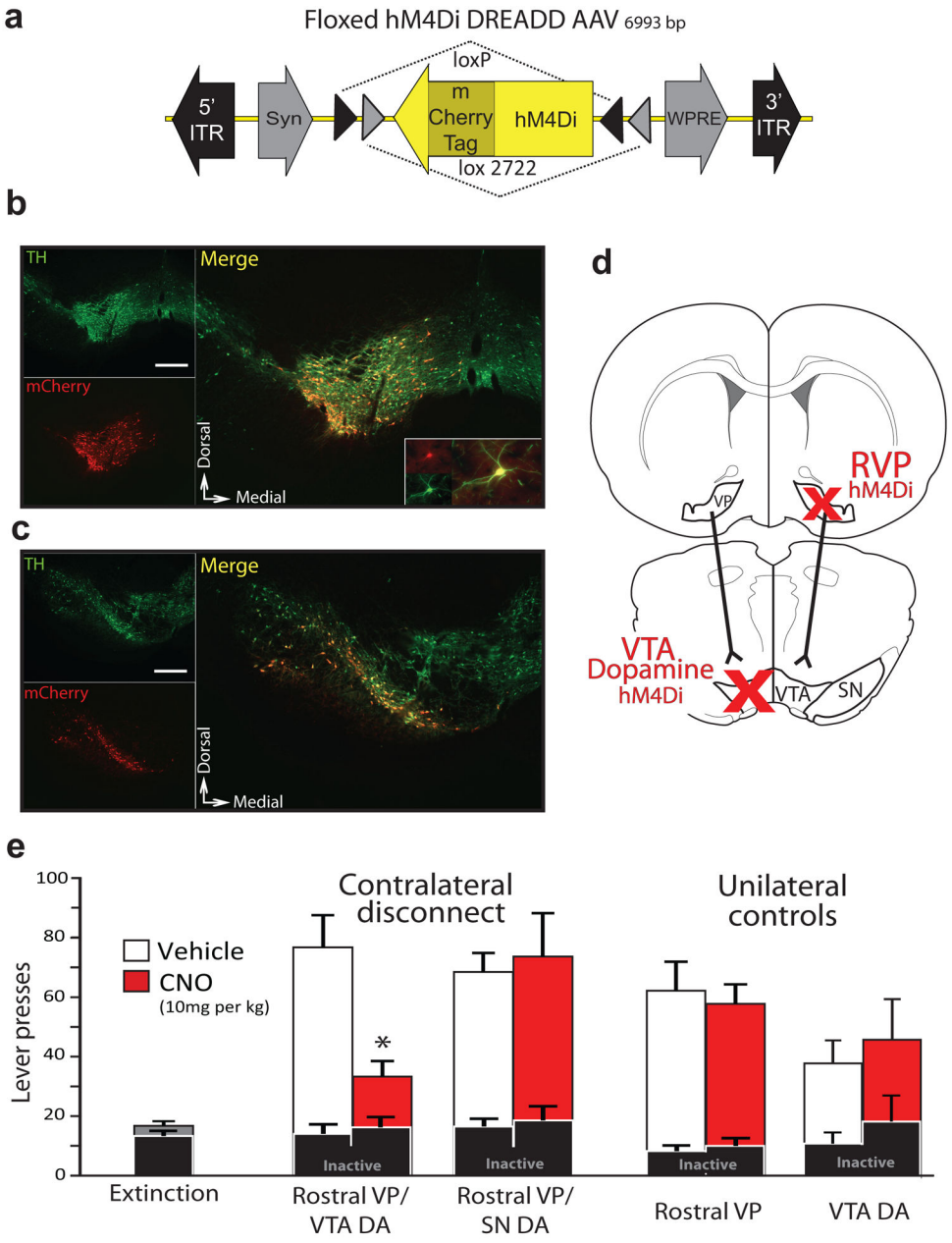

Figure 6. Functional disconnection of rostral VP projection to VTA dopamine neurons blocks cue-induced reinstatement

a) A *DIO-Syn-hM4Di-mCherry* AAV construct was used to selectively express mCherry-tagged hM4Di receptors in dopamine cells in TH::Cre+ transgenic rats. **b)** hM4Di expression is shown in a representative animal with *DIO-Syn-hM4Di-mCherry* injection in VTA. Immunolabeling for TH identifies dopamine neurons (green), and mCherry (red) identifies hM4Di-expressing neurons in VTA. Nearly all hM4Di-expressing neurons were dopaminergic. VTA-injected animals did not show substantial hM4Di expression laterally in SN, or in the contralateral VTA. Scale bar=500 μm. Inset shows hM4Di+TH+ cell at high magnification. **c)** hM4Di expression is shown in a representative animal with *DIO-Syn-hM4Di-mCherry* injections in SN. Minimal expression in VTA was observed. Scale bar=500

μm. Equivalent expression observed in behaviorally tested rats; VTA n=9, SN n=8. **d)** Unilateral S*yn-hM4Di-HA-GFP* injections were made in RVP, and *DIO-Syn-hM4Di-mCherry* injections were made in the contralateral VTA or SN of TH::Cre+ rats, or VTA of Cre- littermates. When systemic CNO is administered, serial connectivity between VP and midbrain dopamine populations is compromised bilaterally via unilateral hM4Di inhibition of RVP, and contralateral hM4Di inhibition of dopamine neurons. **e)** Active and inactive lever pressing during cue-induced reinstatement in RVP/VTA dopamine contralateral disconnect animals. Pressing during late extinction (Ext., grey bar at left), and cued reinstatement after vehicle (white bars) or CNO (10 mg/kg; red bars) are shown. All contralateral disconnect animals received unilateral RVP S*yn-hM4Di-HA-GFP* injections, and contralateral *DIO-Syn-hM4Di-mCherry* injections into VTA or SN of TH::Cre+ rats. Unilateral RVP inactivation rats (RVP hM4Di) were Cre negative, and received unilateral RVP hM4Di virus, plus contralateral VTA dopamine hM4Di virus (though the latter did not cause hM4Di expression in these Cre- rats). Unilateral VTA dopamine inactivation rats (VTA dopamine hM4Di) were Cre+, and received only unilateral VTA dopamine hM4Di virus. Only contralateral disconnection of RVP from VTA dopamine neurons reduced cued reinstatement below control levels. *****$p<0.001$. Bars=m±SEM.

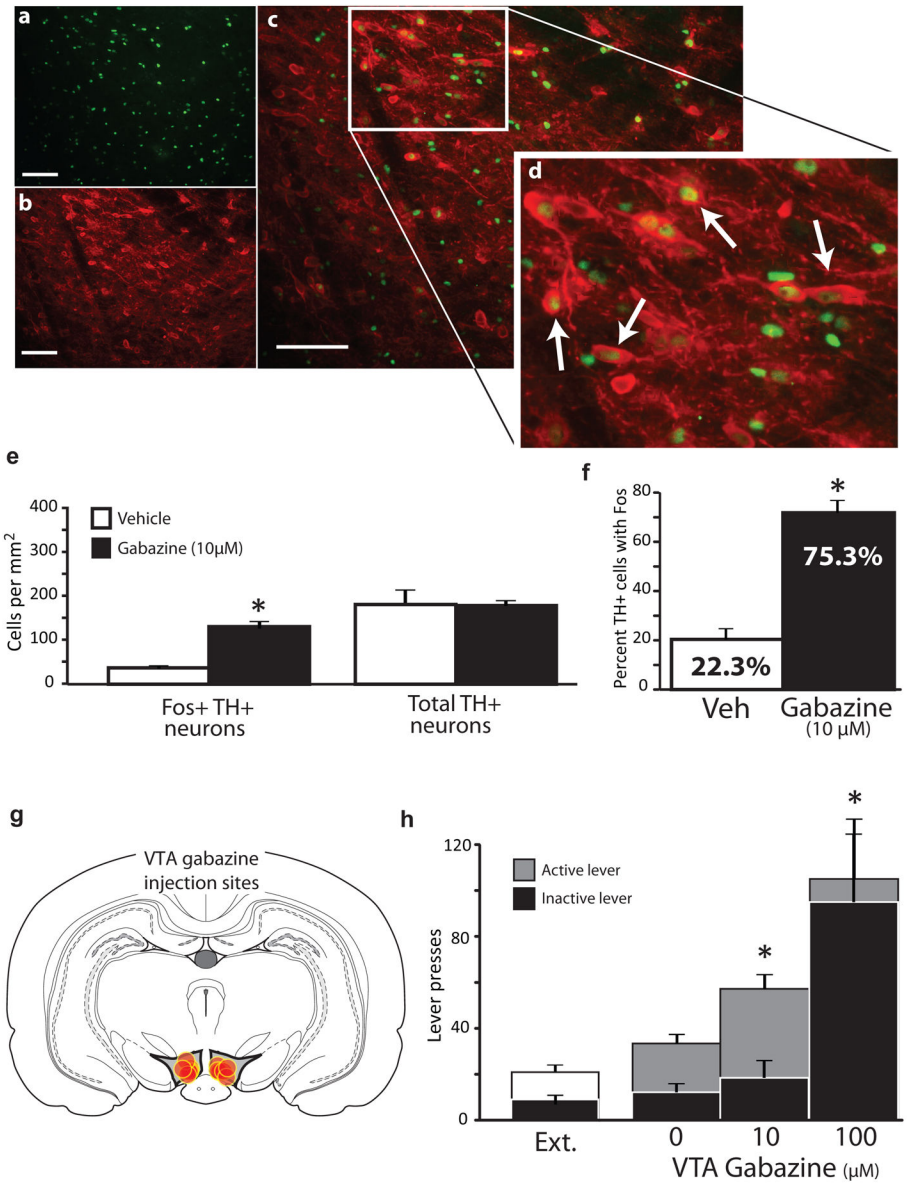

Figure 7. GABA$_A$-mediated disinhibition of VTA dopamine neurons enhances cue-induced reinstatement

a) Example of Fos staining after nearby VTA gabazine microinjection (10 μM/0.3 μl). **b)** Example tyrosine hydroxylase (TH) staining of the same tissue. **c)** Overlay of Fos and TH staining. **d)** Magnified view of Fos+TH overlay. Arrows point to co-labelled neurons. n=5. **e)** Compared to vehicle microinjection, gabazine induced Fos in TH+ neurons, but did not affect the number of TH+ neurons. **f)** Gabazine increased the percentage of TH+ neurons that expressed Fos. **g)** Gabazine injection sites within VTA from cue-induced reinstatement animals. Gabazine was injected at equivalent sites as Fos/TH stained section in panel a. **h)** VTA gabazine (10 μM) increased active, but not inactive lever pressing during cued reinstatement. In a subset of animals, gabazine (100 μM) robustly increased pressing on both

levers, which was very likely related to intense non-specific locomotor activation observed. *p<0.05. Bars=m±SEM. Scale bar=100 μm.